Development of nanostructures using alumina (Al$_2$O$_3$) templates over different substrates for Hydrogen Production

Submitted By

Prof. Udayashankar N K

Professor, Department of Physics

&

Dr. John D Rodney

Post-Doctoral Fellow, Department of Physics

DEPARTMENT OF PHYSICS

NATIONAL INSTITUTE OF TECHNOLOGY KARNATAKA

SURATHKAL, MANGALORE – 575025

May, 2022

INDEX

1. INDRODUCTION

With the advancement of mankind and enrichment of globalization has led to the scarcity of energy (energy crisis) throughout the world. This energy crisis stands as a significant bottleneck in the development of nations and also has a major impact in the economy. It is stated that in the next 60 odd years the fossil fuels will be depleted completely leading to the need for energy source as all our day-to-day lives, work, transportation all currently depends on the fossil fuel [1].
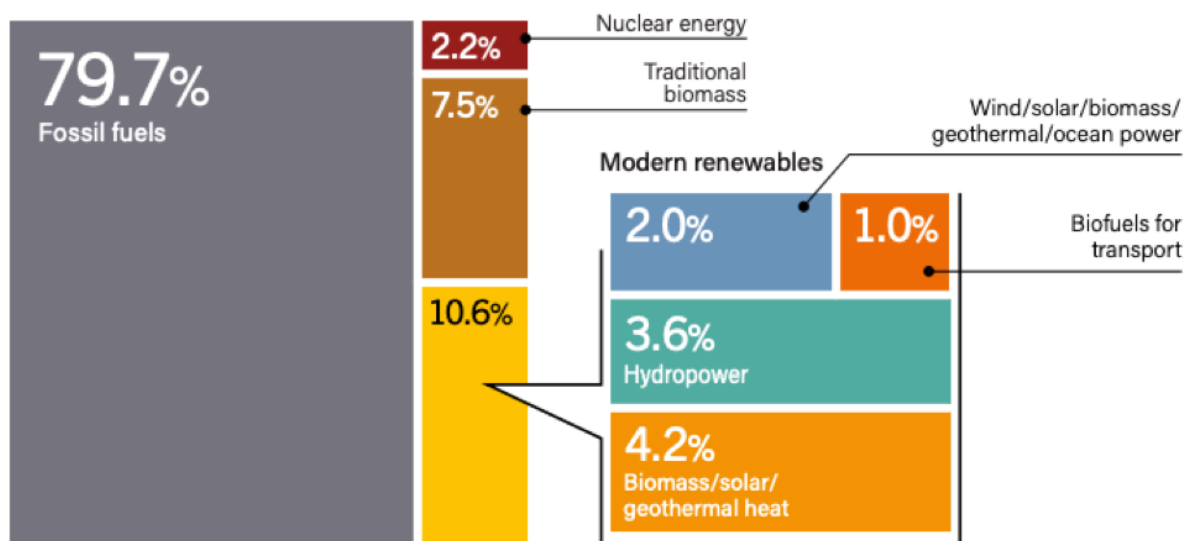
Figure 1 *Estimated Global Renewable Energy Share of Total Final Energy Consumption (2017);*

Source: C2ES

To overcome this pertaining issue the researching community is focused on utilization of the renewable energy sources. And as a result, 20.3% of global energy generated in 2017 is attributed to the renewable energy sources. This potential was only achievable due to the impact of nanotechnology. As it has opened a versatile field of research for the researching community to explore and exploit the true potential of any material with respect to the need of the moment. According to the Centre for Climate and Energy Solutions (C2ES), Arlington, Virginia; due to the intervention of nanotechnology this attribution of renewable energy sources to the global energy production is expected to rise 45% by 2040.

Still to achieve that, the produced energy has to be stored in-order for sustained usage. Yet, it is a never-ending hurdle for the researching community. To satisfy this issue Hydrogen (H_2) is considered as the viable material as it can be used as an ideal source of energy and also a clean energy carrier due to its very high energy density of 142 MJ kg^{-1}. Further, it is eco-friendly and doesn't possess any ill-effects like the carbonaceous fuels. Due to its never-ending properties and advantages the researching community has accepted H_2 as the fuel which can satisfy all the energy-related issues.

Currently, hydrogen production can be carried out by various processes such as water electrolysis (water splitting), photoelectrocatalytic water splitting [2], steam reformation of hydrocarbons, acidic hydrolysis of metal hydrides and reactive materials. Amidst these the water electrolysis or the electrocatalytic water splitting is considered as the most cutting-edge and greater way of producing H_2.

The reason for the selection of electrocatalytic water splitting is because, the hydrolysis method on metal borohydrides, reactive materials is a faster way of producing hydrogen in huge quantities. The source of production is always toxic metals and thus they pollute the environment in a different way. Similarly, the photoelectrocatalytic water splitting is a much greener way of producing hydrogen as it uses the photons directly to produce H_2. Yet, the production amount with respect to other techniques is very low and also it uses only one type of renewable energy (solar) for the production which is a huge downside. Further, the steam reformation of hydrocarbons is a well-known method of producing large amount of H_2 but is not considered here since the hydrogen produced in this method is of lower quality and also contains oxides of C, N and S. Thus, the electrocatalytic water splitting using the energy of the renewable sources is the most proficient way since it is used to convert the renewable energy to H_2 fuel which can be further used as a fuel or also as a energy carrier in almost every day-

to-day application and it is completely eco-friendly since the by-product of burning the hydrogen fuel is water.

2. SCOPE, MOTIVATION & OBJECTIVES

2.1 Scope

AAO template directly grown on a substrate can be used to develop different types of nanomaterial arrays with a controlled morphology that can be targeted for various applications. This stands as a cost effective approach in fabricating a device for any application and it's cost effective due to the lesser need of chemicals for direct growth of nanomaterials in the substrate rather than separate synthesis and then fabricating as a device. With the developed AAO template the LDH@gC$_3$N$_4$ complex can be integrated in a controlled morphology and can be subjected to the production of hydrogen through water splitting. Further, any other materials can also be fabricated in a similar fashion and can be subjected to the production of hydrogen. This technique is highly versatile and productive that the scope can also be further expanded to other various trending applications as stated below.

- **Carbon capture** [3]
- **Photoelectrocatalysis** [2,4]
- **Gas sensing** [5–7]
- **Bio sensing** [8–10]
- **Supercapacitors** [11]
- **Supercapattery** [12]

These applications can also be carried out in addition to water splitting and the versatility of the AAO template on a substrate for the development of nanostructured arrays for diverse applications can be justified.

2.2 Motivation

The present proposal focuses mainly on the development of nanostructures through alumina template for energy applications. Mainly trying to achieve hydrogen production as it is the best alternative to the present fossil fuels and also acts as the best way to store energy generated from renewable energies.

This ability to achieve desired nanostructures directly on the template give a major advantage over other synthesize techniques in achieving best active sites, better surface to volume ratio and better integration with electrolyte and so on.

The template based synthesis of nanostructures is a conceptually simple, cost effective and suitable technique to fabricate nanowires, nanotubes, nanorods and nanofibers. Template based synthesis is a bottom-up approach based on principles similar to those of producing components through the use of replication. These templates contain very small nanoporous channels within the host material and their empty spaces are filled with the required material, which adopts the morphology of pores to form nanostructures. In template assisted synthesis of nanostructures the chemical stability, mechanical properties of the template, pore diameter, uniformity and density of the pores are the important characteristics to consider.

2.3 Objectives

1. To develop AAO template on an ITO/FTO substrate using electrochemical anodization.

2. Try to alter the structure of the AAO template from narrow channels to other various types as mentioned above.

3. Develop various LDH@gC_3N_4 complex (i.e., Ni-Fe LDH@gC_3N_4, Co-Fe LDH@gC_3N_4, Zn-Fe LDH@gC_3N_4) in a controlled morphology and subject them to hydrogen production.

4. Developing nanostructures using the same Substrate based AAO template and achieve various other applications like carbon capture, photoelectrocatalysis, gas sensing, bio sensing, supercapacitors, supercapattery.

5. Publish articles for each application in various high impact factor Q1 journals.

3. EXPERIMENTAL METHODOLOGY AND PROCESS FLOW
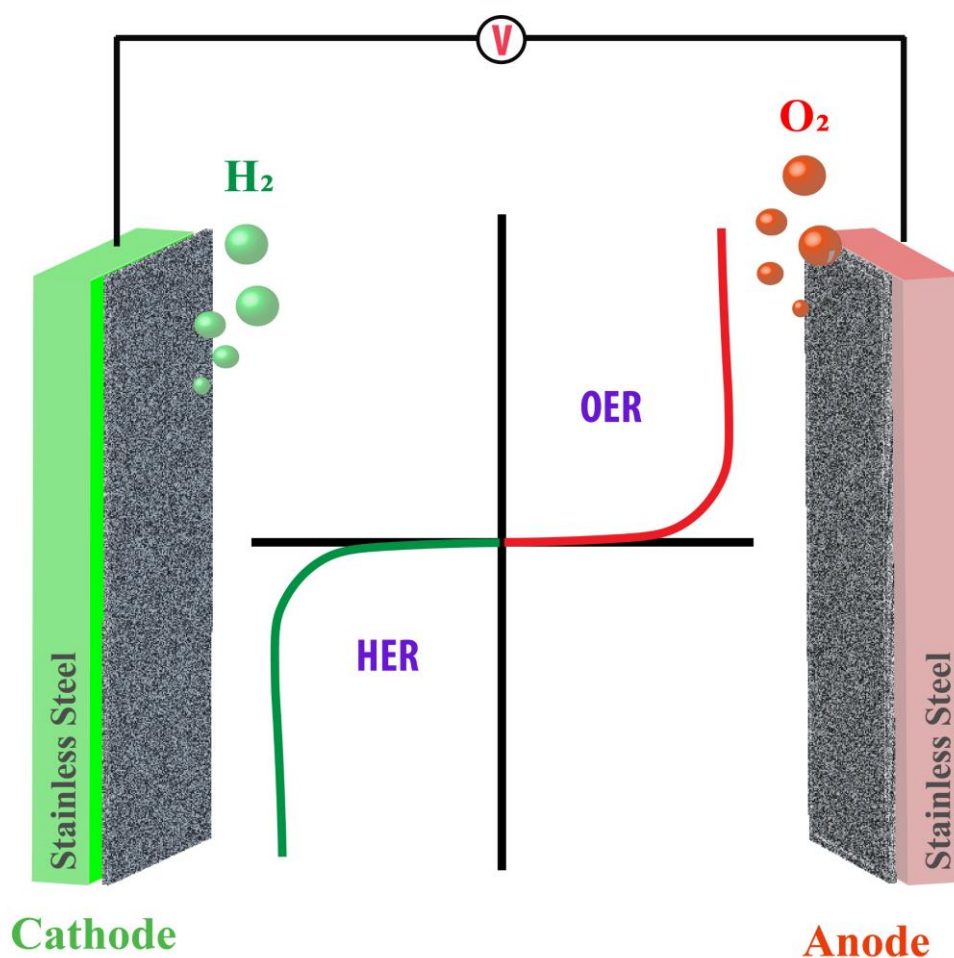
3.1 Water splitting

Figure 2 Bi-functional electrocatalytic water splitting mechanism (for illustration purposes)

The Fig. 2, showcases the standard electrolytic cell setup with an anode and cathode in an electrolyte. When an external voltage is applied in between the electrodes HER and OER

occurs at the cathode and anode respectively. The process of water splitting changes with respect to the electrolyte used (acidic or alkaline). Eqn. (1 – 5);

$$Total\ reaction\ H_2O \rightarrow H_2 + 1/2O_2 \tag{1}$$

In neutral or alkaline solution

$$Cathode\ 2H_2O + 2e^- \rightarrow H_2 + 2OH^- \tag{2}$$

$$Anode\ 2OH^- \rightarrow H_2O + 1/2O_2 + 2e^- \tag{3}$$

In acidic solution

$$Cathode\ 2H^+ + 2e^- \rightarrow H_2 \tag{4}$$

$$Anode\ H_2O \rightarrow 2H^+ + 1/2O_2 + 2e^- \tag{5}$$

At present, most of the conveyed bi-functional electrocatalyst are operated on alkaline electrolyte rather than an acidic medium, for it gives an option for the replacement of noble metal electrocatalyst such as platinum [13], iridium [14], ruthenium [15] with cost-effective transitional/functional based electrocatalysts. Further, they assist O_2-evolution process thus allowing a faster reaction kinetics than in an acidic medium. In general, the thermodynamic voltage for splitting water is 1.23 V (25°C and 1 atm), thus, in-order to conduct water splitting in real-time requires more voltage than the theoretical standards and this is known as the operating voltage (V_{op}); Eqn. 6;

$$V_{op} = 1.23\ V + \eta_a + |\eta_c| + \eta_\Omega \tag{6}$$

Here, η_a and η_c, are the overpotentials essential to overawed the fundamental activation barriers in the anode and cathode of the cell respectively. η_Ω exhibits the extra potential required to overcome the solution and internal resistances. Thus, the electrocatalyst also stands as an integral challenge to develop an exceptional bifunctional water splitting setup for pure and long-standing hydrogen production. To understand in-depth, the active in each electrodes OER and HER are briefly explained as follows.

3.2 Oxygen Evolution Reaction (OER)

Considering the two evolution reactions occurring in the system, OER is considered to be the much complex mechanism when compared to HER. For, lot of parameters play a vital role in the reaction kinetics of the electrode and the anode (OER electrode) is considered to be the vital part of the splitting system. O_2 usually evolves from the M-O surface rather than from the bare surface thus the reaction mechanism varies for similar oxides with varied structural composition and in addition even the reaction kinetics of the same compositional material will vary due to the difference in coating or deposition thickness and different preparation procedure.

For an oxide material, in-general, the anticipated mechanism is as follows; Eqn. (7 – 11);

$$M + H_2O \rightarrow MOH + H^+ + e^- \tag{7}$$

$$MOH \rightarrow MO + H^+ + e^- \tag{8}$$

(or)

$$2MOH \rightarrow MO + M + H_2O \tag{9}$$

$$2MO \rightarrow 2M + O_2 \tag{10}$$

(or)

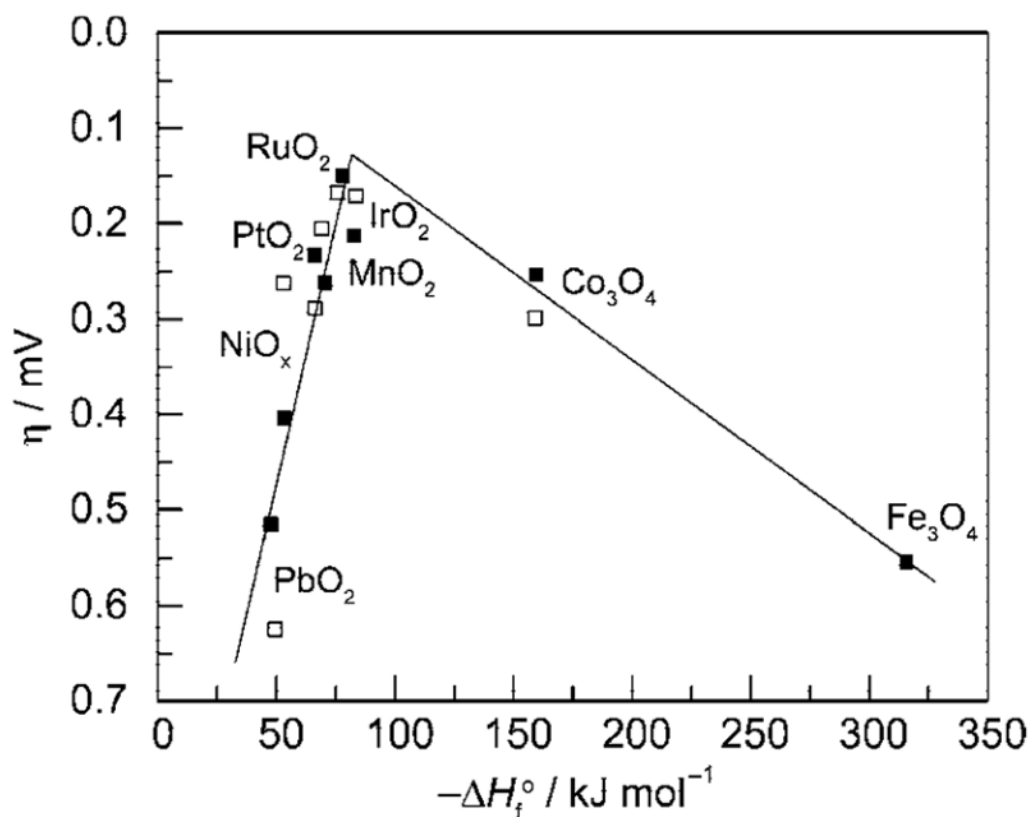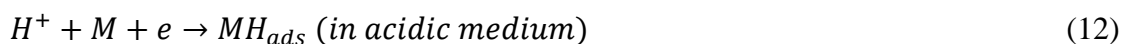$$MO + H_2O \rightarrow M + O_2 + 2H^+ + 2e^- \tag{11}$$

Figure 3 *Volcano plot showcasing the oxygen production activity over a metal oxide surface vs enthalpy of transition of the oxide in acidic (dark spot) and basic (light spot) solutions.*
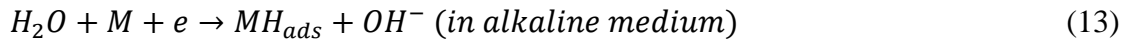
From Fig.3, we can see the activity of oxygen generation by various transition metal oxides in acidic or basic conditions. The noble metal oxide is placed at the top of the peak since they possess great electrical conductivity and very low redox potential. But their higher cost and low HER activity makes them ineligible as a bi-functional electrocatalyst. Thus, a need for a better OER material which is also cost-effective is required.

3.3 Hydrogen Evolution Reaction (HER)

The most research part of the water splitting and also the most important section of the splitting too is the Hydrogen Evolution Reaction. The HER process consists of 3 steps alkaline and acidic media;
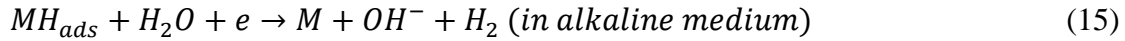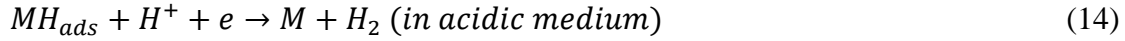
Volmer reaction (electrochemical adsorption) Eqn. (12, 13);

$$H^+ + M + e \rightarrow MH_{ads} \; (in \; acidic \; medium) \tag{12}$$

$$H_2O + M + e \rightarrow MH_{ads} + OH^- \; (in\ alkaline\ medium) \tag{13}$$

Followed by

Heyrovsky reaction (electrochemical desorption) Eqn. (14, 15);

$$MH_{ads} + H^+ + e \rightarrow M + H_2 \; (in\ acidic\ medium) \tag{14}$$

$$MH_{ads} + H_2O + e \rightarrow M + OH^- + H_2 \; (in\ alkaline\ medium) \tag{15}$$

(or)

Tafel reaction (chemical desorption) Eqn. 16;

$$2MH_{ads} \rightarrow 2M + H_2 \tag{16}$$

The Tafel [16] is an important parameter in understanding the mechanism of the HER (cathode) electrode, where the logarithmic overpotential is related to its equivalent current densities (j) and the linear slope is given as the following derivation; Eqn. 17;

$$\eta = a + b \log(j) \tag{17}$$

Where b is the Tafel slope which is related to the electrode's reaction kinetics. When $\eta=0$, the current obtained is called the exchange current density (j_o).

The above-mentioned mechanisms and the electronic configuration of the chosen material play a vital role in the evolution of hydrogen for these are rate determined steps, which will suggest if the activity is due to reaction kinetics or due to mass transport mechanism.
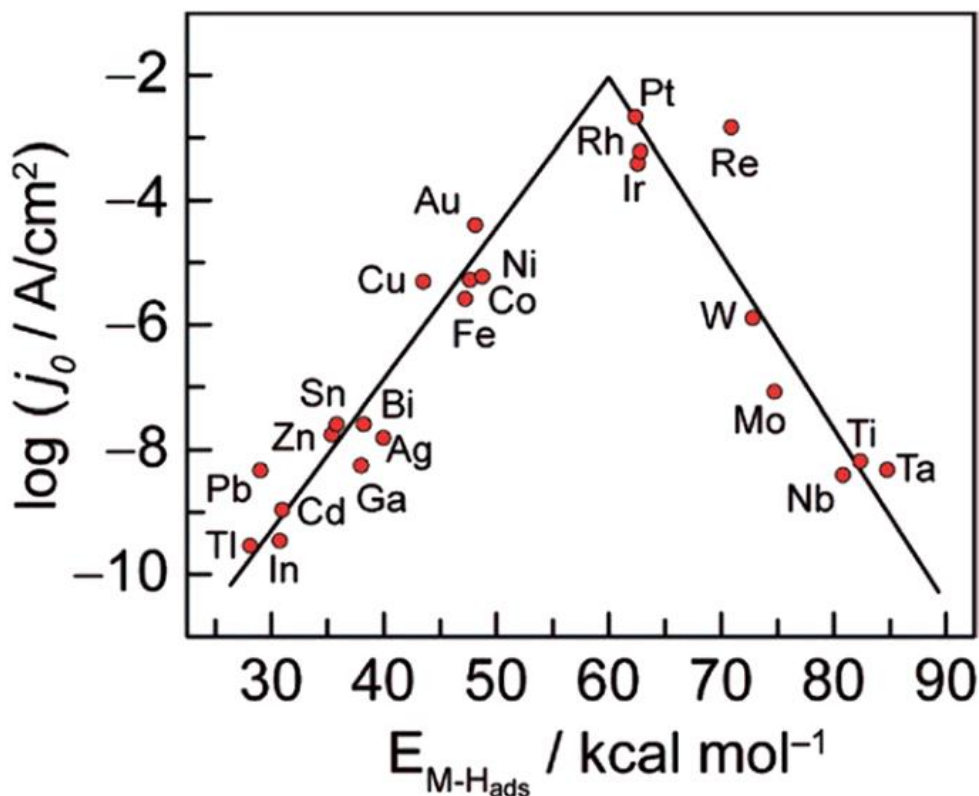
Figure 4 *Volcano plot showcasing the hydrogen production activity over a metal electrode's in acidic medium.*

Fig. 4, depicts the plot for log of the exchange current density vs the M-H bond energy for each metal surface, this confirms the fact that the HER depends of the materials electronic structure. Further in addition, the HER electrocatalyst showcase better performance in acidic electrolyte because of the presence of the excess proton in the medium. Whereas, in an alkaline electrolyte the HER electrode will depend on the OER electrode for the proton since the alkaline electrolyte will have a deficit of protons.

Thus, while developing an ideal bi-functional electrocatalyst for electrocatalytic water splitting not only the development of OER-HER electrocatalyst bring about expected result but other parameters also play a major role such as;

(i)   Capability to work at lower over-potentials with higher current density

(ii)   Ability to incorporate cost-effective earthly abundant materials rather than noble/precious materials

(iii)   Lenience for a wide range of pH.

(iv)   Swift and simpler preparation and fabrication

(v)   Long-term stability

Not all electrocatalyst will satisfy all the required parameters, thus, balancing of efficiency in-between the OER and HER catalyst are very important in a water splitting setup to achieve a larger-production of hydrogen.

3.4 Water resources

In general, the electrolytic medium used for an electrochemical water splitting are the acidic and the alkaline medium with the latter been the prominent choice. It is seen that the fresh water is hugely considered by the researching community to run various experiments to determine the stability and productivity of the OER-HER electrode. Further, the low stock of fresh water has put a huge strain on the fresh-water electrolysis and stands as a hurdle for the commercialization of the water splitting. Only 3% of the overall water is fresh water, even though 70% of the earth is covered with water, in addition, out of the 3% fresh water one-third of it is frozen in the glaciers. Seawater is the most plentiful feedstock of natural electrolyte present on the earth accounting to a 97% of the total water resources in our planet. No advanced desalination process is required for the seawater as the salts in seawater stand critical for they tend to act as charge carriers with high electrical conductivity of 33.9 mScm^{-1} at 25 °C during electrolysis [17].

3.5 Electrocatalyst

Electrocatalyst stands-out to be the most important part of the water splitting. For the past few decades various electrocatalytic materials were examined by the researching communities such as metal oxides [18], metal selenides [19], metal phosphides [20], metal dichalcogenides

[21], metal nitrides [22] and so on. An electrocatalyst is a nanomaterial that initiate the OER/HER process acting as the anode or the cathode or as both anode and cathode in bifunctional catalyst in a water splitting cell. As mentioned above the OER-HER electrode has to satisfy various parameter to act as a prime electrocatalyst for the application. Further, for splitting of seawater additional more parameter is needed to be overcome such as the Chlorine Evolution Reaction (CER) [17], electrode poisoning and so on. In the past years, works were carried out in Co_3O_4 [2], porous manganese-based electrode [23], $TiO_2@g-C_3N_4$ [24], $VS_2@V_2C$ [25], Mn-Mo-W@Ti/IrO_2 [26], NiRuIr_G [27], RuCoMo$_x$ [15] suggesting that only a small amount of progress is carried out in overcoming the pertaining issues in seawater splitting. Recent works have been carried out by Y.Kuang et. al [28] in the development of NiFe/NiS$_x$ over a nickel foam as anode when paired with Ni-NiO-Cr_2O_3 in a two-electrode setup. The cell achieved 400 mAcm^{-2} in 2.12 V in an electrolytic solution of real seawater + 1 M KOH at 23°C with 100% retention capability with no signs of corrosion. Similarly, L. Yu et.al [29] fabricated NiFeN@NiMoN/NF as anode when paired with NiMoN in a two-electrode setup, the cell was able to achieve 1000 mAcm^{-2} for a cell voltage of 1.709 V in overall alkaline seawater splitting at 60°C.

Amidst the above mentioned materials, Layered Double Hydroxides and graphitic Carbon Nitrides (LDH & g-C_3N_4) is considered for they are more constant with a strong ionic bond, with the intrinsically substantial of its s-orbital for they hold high thermal and chemical stability [30]. The inadequate filling of the d-shell constitutes the material with augmented electrocatalytic properties, high dielectric constant, narrow band gap, enhanced electrochemical behaviour with a swift electrical conductivity making them an outstanding material for this process [31]. Various OER and HER activity analysis for a LDH and g-C_3N_4 complex has been carried out separately for the past few decades, whereas, a combined

complex approach and the bi-functional electrocatalytic splitting of seawater using a LDH and g-C₃N₄ complex electrocatalyst stands as a first in its segment.

3.6 Development of electrocatalyst

For an electrocatalyst the synthesis technique stands as a major parameter in deciding the porous nature, particle size, morphology and structural composition of the material. Various techniques were subjected for the synthesis for LDH and g-C_3N_4 respectively. Namely, solvothermal, hydrothermal, solution combustion, sol-gel, co-precipitation, thermal decomposition and so on. But, for developing an electrocatalyst directly on substrate a template based approach is highly accepted.

3.6.1 *Development of Anodic Alumina Oxide (AAO) and grow nanomaterials directly on a substrate*

 Commercial ITO/FTO substrates (Merck) consist of a 180 nm thick ITO/FTO layer deposited on soda-lime-silica glass (1 cm × 2 cm × 2.3 mm). The substrates were first cleaned with dishwashing detergent, and then in an ultrasonic bath for 10 min each with acetone and isopropanol prior to loading in the sputtering system. Physical Vapour Deposition (PVD) technique was used to deposit Aluminium (Al) over the ITO/FTO substrate for a thickness ranging from 600 nm – 1.5 µm under high vacuum conditions. Further, to form AAO template anodization was carried out in a smaller scale considering the minimal thickness of the aluminium on the substrate.
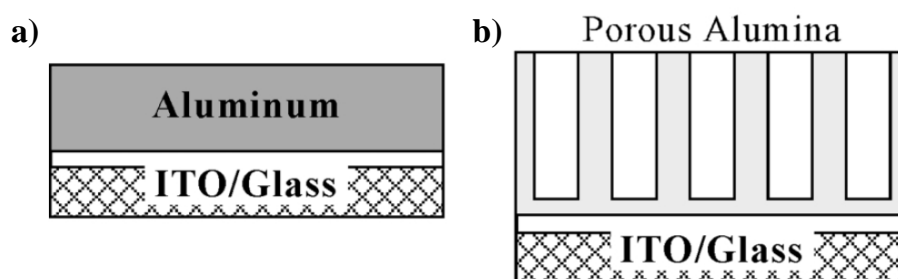

***Figure 5** Scheme of fabrication procedure of nanostructures on ITO/glass substrates. (**S.Z. Chu et al. / Surface and Coatings Technology 169 –170 (2003) 190–194**)*

Anodization was carried out at 5°C using a two electrode system in a jacketed beaker cooled by a recirculating chiller. The samples were installed in a homemade electrode holder with 1×1 cm of coated section dipped into 0.1 M oxalic acid (Sigma-Aldrich). The samples were contacted with crocodile clip in one end. A Keithley 2400 Source Meter supplied the constant anodizing potential, and a platinum foil ring counter electrode was placed in parallel to the Al film at a distance of 1–2 cm. The current was monitored throughout the anodization process.
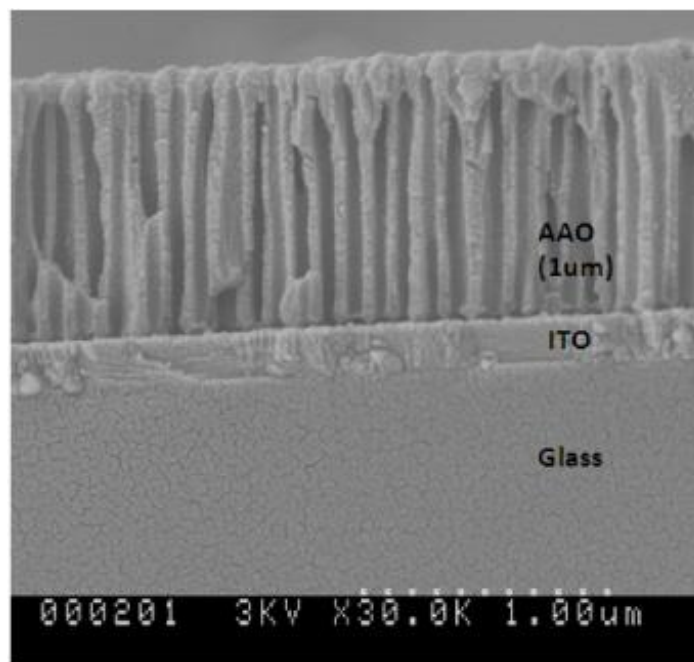

Figure 6 *Cross-section image of a barrier-free template with an AAO thickness of 1 μm fabricated on the glass/ITO substrate. (**P. Liu et al. / Nanotechnology 21 (2010) 115303**)*

As the pores reached the bottom of the Al, the sample turned transparent. When vigorous gas bubbles uniformly spread out from the sample surface, the anodization was manually stopped. It is important to stop the anodization process at the proper point because the barrier layer needs to be thinned for a sufficient duration, but the process should not be too long as this would damage the film. The alumina barrier layer was subsequently completely removed in 5 wt% phosphoric acid (Sigma-Aldrich) at room temperature while the AAO pores widened. So of the materials developed through this technique is as shown below.
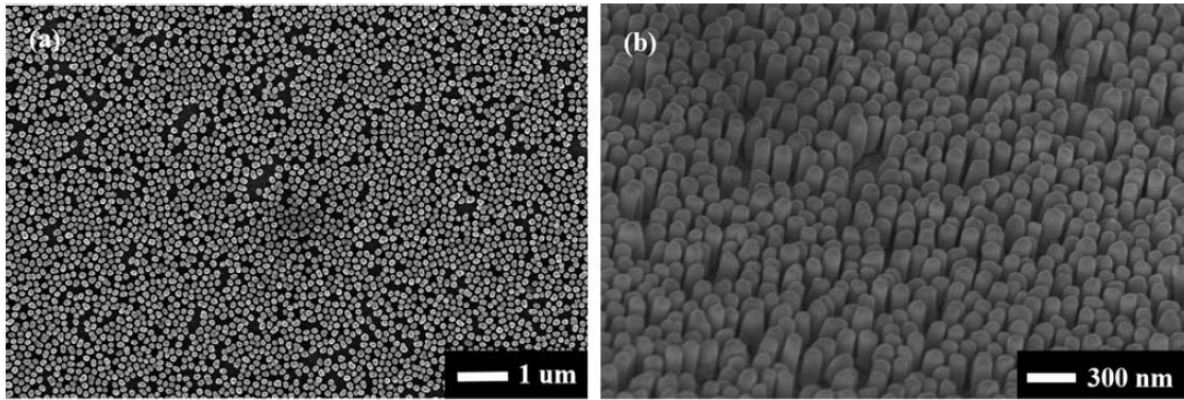
Figure 7 *SEM images of free-standing silver nanowires on ITO glass substrates: (a) top view, (b) side view at an angle of 54∘.* ***(Yuyi Feng et.al. / Journal of The Electrochemical Society, 163 (8) D447-D452 (2016))***
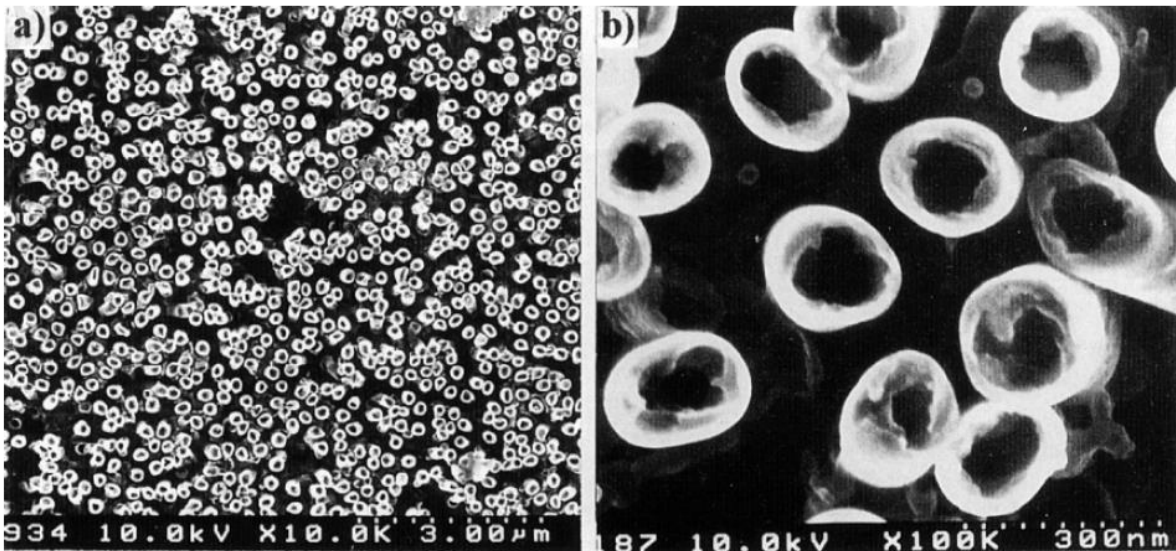
Figure 8 *Titania nanotubules array standing on an ITO/glass substrate.* ***(S.Z. Chu et al. / Surface and Coatings Technology 169 –170 (2003) 190–194)***

With respect to Fig. 6-8, it can be clearly seen that the AAO templates can be directly developed onto a substrate and required Nano rods / Nano tubular arrays can be developed over a substrate without any intermediate process. This in turn completely develops that scalability of the nanomaterial's as this increases the surface to volume ratio and developed the activity of the materials.

3.7 Modification to the AAO template structure

Rather than developing materials with the narrow shaped AAO template, works are being carried out to develop various structures for the development of highly active and responsive nanomaterials. When the AAO templates internal shape is varied the nanomaterial deposited or grown tend to follow that structure. There are various way of modifying the AAO template as listed down.
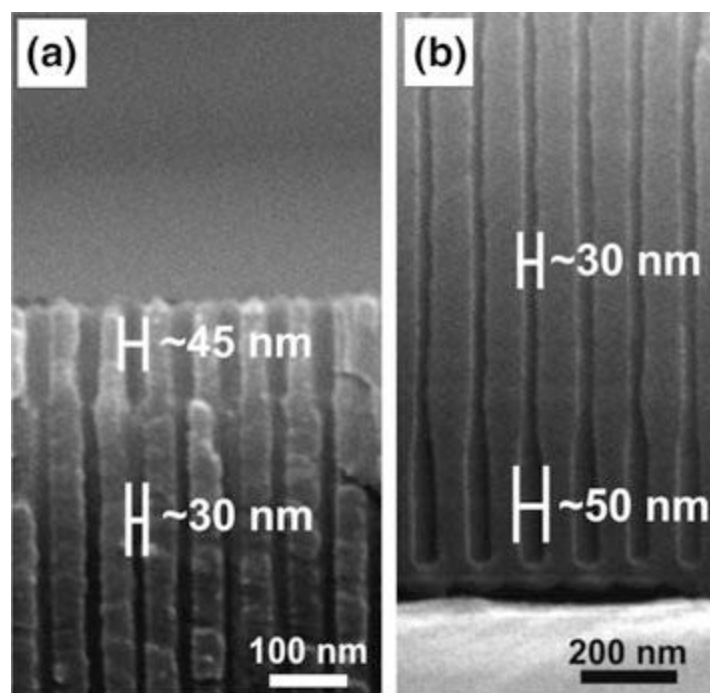
3.7.1 AAO with Step-Shaped Nanochannels

Figure 9 *SEM images of AAO layers with step-shaped nanopores **a**) formed by 10 min of anodization in 0.3 M H₃PO₄ followed by 5 min anodizing in a 0.3 M H₂C₂O₄, and reversed step-shaped nanopores **b**) formed after changing the order of the used electrolytes. All anodizations were carried out at 45 V and 20°C*

A procedure, consisting of two MA processes carried out at the same voltage and separated by chemical etching, was used for fabrication of AAO films with step-shaped nanochannels (Figs. 9 a) & b). On the other hand, by combination of MA and HA processes the step-shaped pores can be also created when the pre-patterned Al substrate is anodized. The step-shaped nanopores in AAO might be successfully formed by a potentiostatic anodization with an anticipated exchange of the anodizing electrolyte. At the beginning of the process, phosphoric acid with a lower pH is used, then oxalic acid is poured into the cell. The step-shaped nanopores can be

also created after the anodizing voltage increase for a very short time by a factor of $\sqrt{3}$. The pore narrowing after voltage increase was attributed to the enhanced activity of H^+ ions at the original pore bottoms.

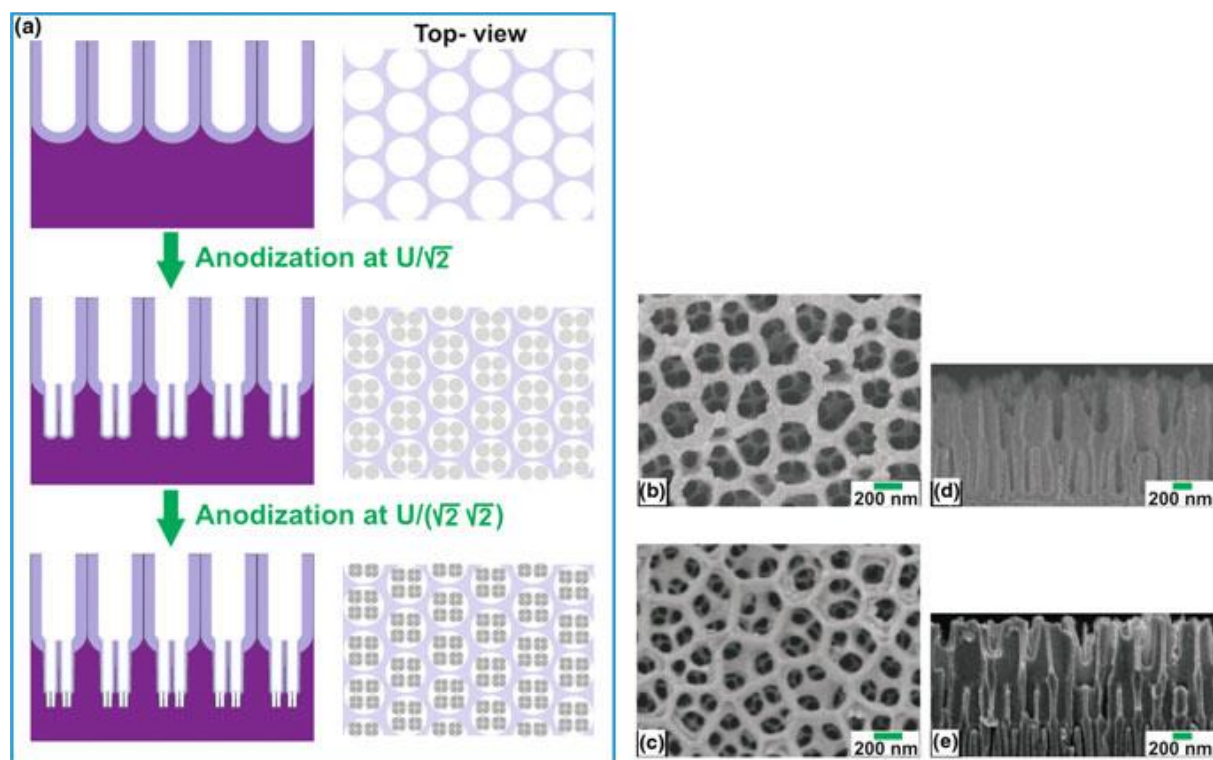### 3.7.2 *AAO with Step-Shaped Nanochannels*

***Figure 10 a)** Schematic for fabrication of multilevel Y-branched nanopores in AAO by a sequential reduction of anodizing potential. Top (**b** and **c**) and cross-sectional (**d** and **e**) SEM images of AAOs formed by anodization with a single (**b** and **d**) and double (**c** and **e**) reduction of anodizing potential by a factor of $1/\sqrt{2}$. The initial anodization was carried out in 0.3 M H3PO4 at 130 V for 35 min, the barrier layer was thinned for 150 min in 5 wt% H3PO4. After the first reduction of potential (**b** and **d**), anodization was performed in 0.15 M C2H2O4 at 80 V for 3.5 min, and the barrier layer was thinned for 90 min. After the second reduction of potential (**c** and **e**), anodization was performed in 0.3 M C2H2O4 at 50 V for 15 min, and the barrier layer was thinned for 40 min. (**Ref. Copyright 2008 WILEY VCH Verlag GmbH & Co. KGaA, Weinheim**)*

Most of the studies on AAO templates have been focused on fabricating linear nanopores in the alumina films. Recently, AAO templates with more complex-shaped nanopores were successfully synthesized by anodization. Since the cell diameter of porous anodic alumina is proportional to the anodizing voltage, reducing the applied voltage by a factor of $1/\sqrt{2}$ results in twice as many pores appearing on the surface. Consequently, nearly all pores branch into two smaller diameter pores (a symmetrically divided Y) in order to maintain the original total

area of the template. Therefore, the AAO layer with Y-branched nanopores (Fig. 10) can be obtained by reducing or increasing the applied anodizing voltage by a factor of $1/\sqrt{2}$ and by anodization of aluminum in two different electrolytes, i.e., in oxalic acid at 40 V and then in sulfuric acid at 25 V or in oxalic acid at 40 V and then phosphoric acid at 80 V.
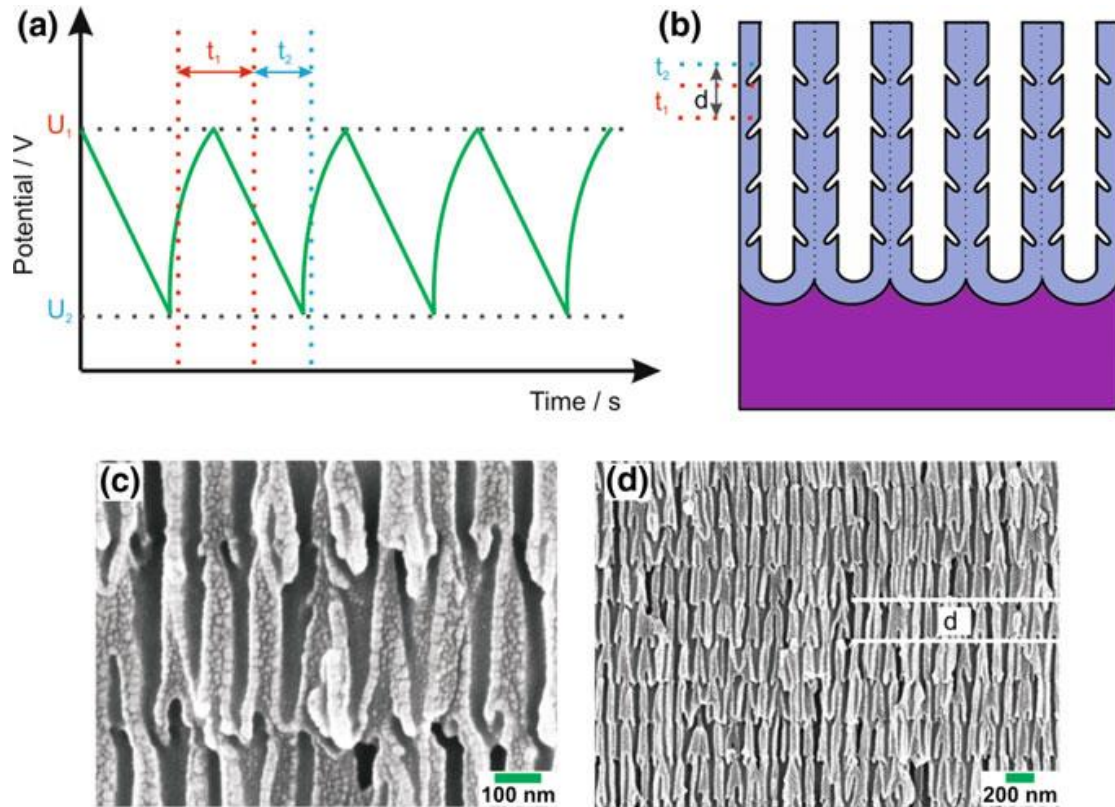
3.7.3 *AAO with periodically branched Nanochannels*

Figure 11 Schematic illustration of the typical voltage signal applied during the periodic anodization of aluminum a) together with the formed AAO layer b). The cross-sectional SEM images of prepared AAO layers with periodically branched nanopores (c and d). The anodization was carried out at 18 °C in 0.3 M oxalic acid. The applied anodizing potential decreases linearly from 53 V to 23 V in 2.5 min, and then increases sinusoidally from 23 V to 53 V in 15 s. The thickness of the single layer (d) was about 290 nm. (2009 Chinese Physical Society and IOP Publishing Ltd)

A potentiostatic anodization with periodic changes in the anodizing voltage or current density was used for the fabrication of periodically branched nanoporous structures (Fig. 11). Figure 11 shows the schematic illustration of the typical voltage signal applied during the periodic anodization of aluminum together with the grown AAO structure and SEM cross-sectional view images of the AAO with periodically branched nanochannels.

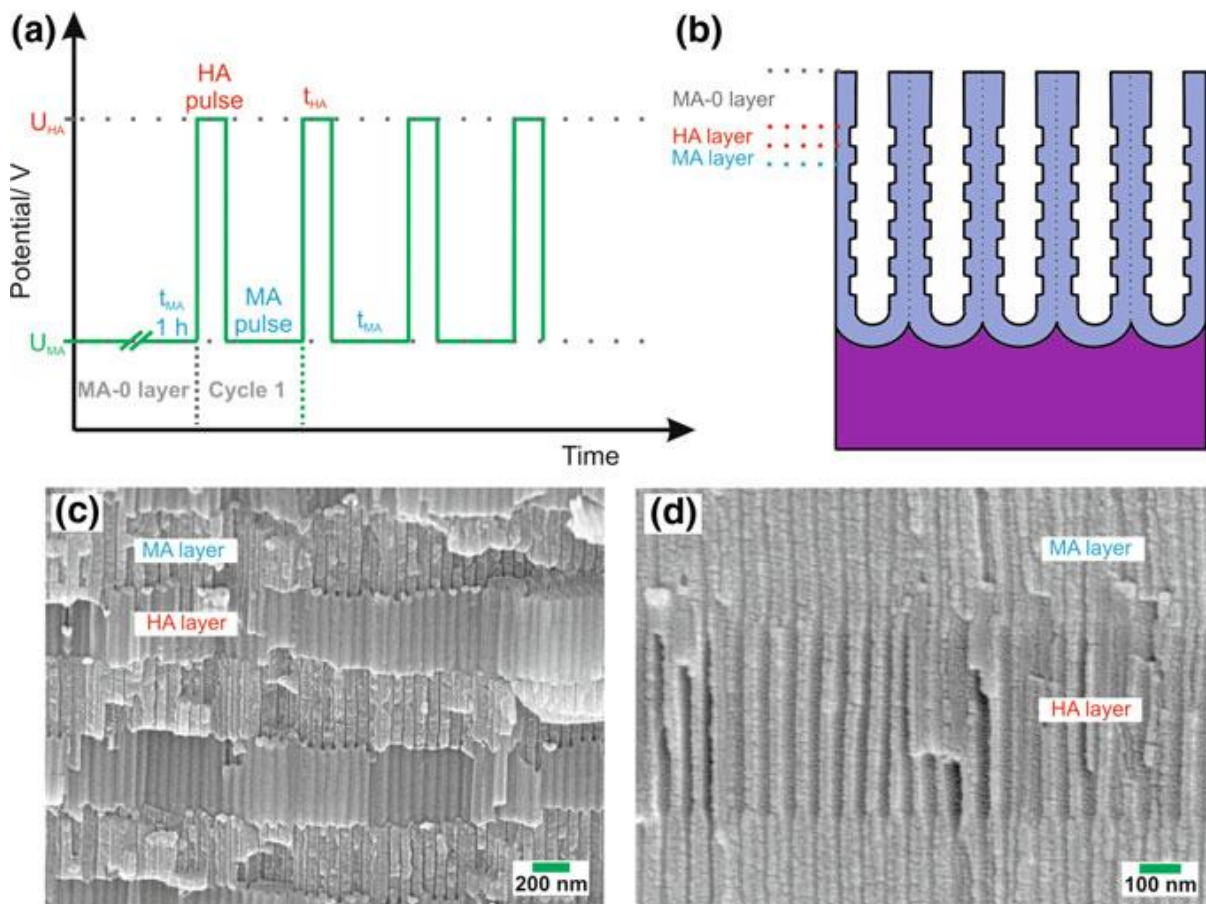### 3.7.4 *AAO with Modulated Pore Diameters*

Figure 12 *Pulse anodization of aluminum for pore diameter modulations. **a)** A typical voltage signal applied during the pulse anodization of aluminum, where U_{MA} and U_{HA} are the anodizing potentials used to achieve mild anodizing (MA) and hard anodizing (HA) conditions, respectively. **b)** A schematic representation of the AAO structure with a modulated pore diameter grown after a few HA and MA pulses. **(c and d)**The SEM cross-sectional views of AAOs with modulated pore diameters by pulse anodization in 0.3 M H_2SO_4 at 1°C. Each cycle consisted of the MA pulse ($U_{MA} = 25$ V, $t_{MA} = 180$ s) and HA pulse ($U_{HA} = 35$ V, $t_{HA} = 0.5$ s)*

Over the past decade, AAO templates with periodically modulated pore diameter (Fig. 12) have been synthesized by: (a) pulse anodization that combines subsequent mild anodization (MA) and hard anodization (HA) processes performed at different voltages or different current density, (b) hard-pulse anodization technique that combines two different HA potential pulses, (c) pulse changes of electrolyte flow, (d) anodization in sequentially changed electrolytes but at the same anodizing current density or anodizing potential.

3.8 Additional innovative research works

Some snippets of innovative work that can be carried out if the above mentioned equipment's are been purchased.

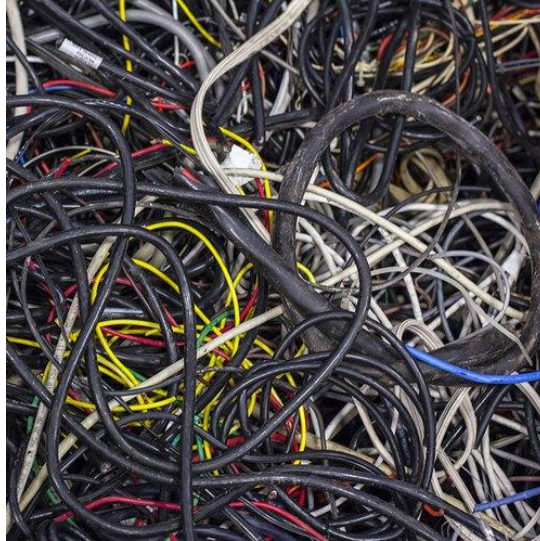**3.8.1 _Energy harvesting and storage using used copper wires_**

Figure 13 *Waste/disposed copper wires*

Copper wires are the widely used material in our day to day lives in every possible parameters. Copper comes from two sources: extraction and processing (refining) of raw materials, called primary production; and recycling of end-of-life products, called secondary production. In the last decades, the world mining production of copper has grown by 3.2% per annum to 20 million tonnes in 2017 and its largest producer was Chile (5.6 million tonnes). The total global demand for copper in 2016 was approximately 25 million tonnes and China was its largest consumer with nearly 12 million tonnes. Copper is one of the most recycled metals. It is estimated that in 2016, about 29% of the copper used came from recycled copper and around 40% of the demand for copper within Europe was supplied from recycled copper.

Thus copper wire are widely and abundantly present and are being recycled and used continuously.

Currently, in the field of water splitting, supercapacitor, battery and supercapattery highly sophisticated and costly working electrodes are used as an electrode in which the nanomaterials are grown or deposited for further applications. Some of the working electrodes namely Ni Foam, Ni Sheet, Glass Carbon, Carbon Cloth, Carbon Foam, Carbon Mesh and so on. These materials are very costly and are a problem when we consider large scale production or storage. Thus, in an innovative way if we could obtain the waste/disposed copper wires, clean them through mild acid treatment and then deposit our desired materials through drop-casting or any other approach over these copper wire and then subject them to water splitting, supercapacitor, battery and supercapattery, which will make it an innovative approach in reducing the cost of working electrodes and also paving a way for commercialization.

This type of wok can bring about high impact factor article in a Q1 journal, but can only be achieved if the above requested equipment can be purchased.

3.8.2 *Energy harvesting and storage using used car/bike tyres*

Even as India struggles to manage its plastic waste, a new report has raised concerns about the impact of generating a cheap and polluting fuel from used tyres in pyrolysis plants.

The Guardian reported that, every month, the UK exports "thousands of tonnes" of used tyres to India. It suggests that most of these tyres are used by pyrolysis plants to produce fuel. Several of these plants flout regulations on pollutants released in the process.

In 2014, the National Green Tribunal banned the burning of used tyres in the open or using them as fuel in brick kilns, because they produce toxic smoke known to be hazardous to health. Though the petition was brought before the tribunal to end burning of tyres during protests, it took a wider view of the problem. It asked the Maharashtra Pollution Control Board (MPCB) to look at ways to dispose used tyres safely.

Figure 14 Disposed car tyres (Left); tyre schematics (Right)

As with most pollutants, experts suggest that though recycling is imperative, the ultimate goal should be a reduction of usage. In India, tyre production has been on the rise and is expected to grow at a rate of 7-9% over the next five years. If guidelines on recycling the tyres continue to be ignored, the air pollution crisis in India will only become worse.

In such a way, the steel belts inside the car/bike tyres can be savaged and the rest of the tyre can be subjected to pyrolysis (thermal decomposition) and be reused.

The steel belts obtained from the used tyres can be made as a rod or as any desired shape and can be cleaned to remove any possible contamination left, then this obtained steel can be further used as the working electrode over which the electrocatalyst will be grown or deposited and application based studies for water splitting, supercapacitor, battery and supercapattery can be carried out. These will bring about highly innovative results which can be compared with currently commercialized materials and can be proven as a best suitable replacement for the costly materials.

This work only can be carried out if the above mentioned equipment's are available and highly sophisticated papers can be published with respect to this topic.

3.8.3 *Seawater splitting*
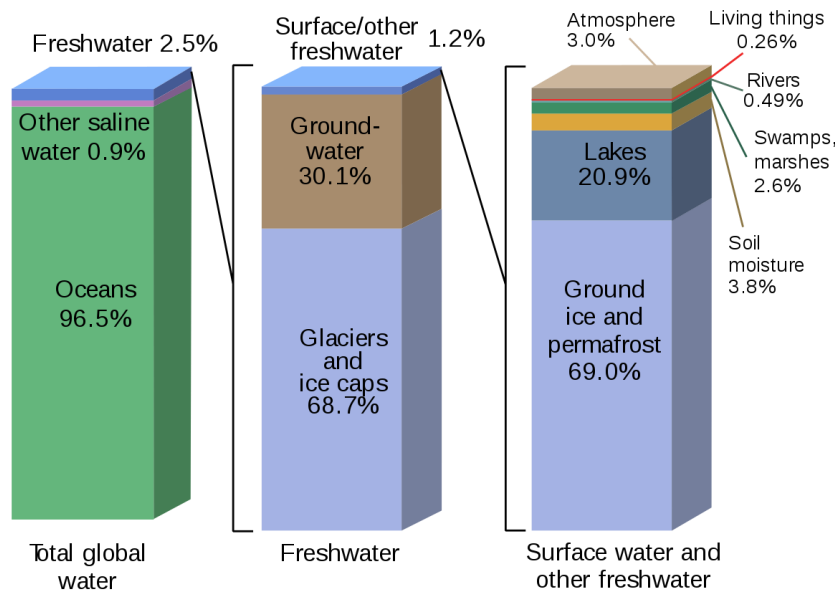
Where is Earth's Water?

Figure 15 Global Water ratio split-up (graphical)

This is one of the objective for this project. Currently only fresh water splitting is being carried out in a vast manner. But the depletion of fresh water sources stands as a bottle neck in achieving mass production of hydrogen as fuel or energy storage source. This way we can concentrate on producing hydrogen through seawater obtained from the NITK beach (Arabian sea) and various studies can be carried out with respect to that can the possible issues of chlorine corrosion, electrode poisoning due to sea water can be eradicated and a better output can be achieved. Further, the above mentioned copper wire and steel rods from tyres can also be subjected to this research and highly innovative research output can be obtained.

This will be a novel type of research done and the first research activity from India, where we used waste copper wire or steel from tyres to produce hydrogen from sea water. This concept will be highly accepted and High impact paper can be achieved and this research activity will also bring laurels to the department and the institution.

The addition advantage is, we also have a post-doctoral scholar who has vast experience in these applications and has also published a first of its kind seawater splitting paper using stainless steel sheets as electrodes to splitting sea water from Bay of Bengal [32]. Thus, if the equipment's can be procured the possibility of achieving this research output is very high.

4. REQUIREMENTS

To achieve this project and to bring about various applications along with articles in reputed high impact factor Q1 journals, there are couple of equipment's required.

This required equipment's along with their information and justification is given below.

4.1 <u>Keithley Potentiostat</u> (2450-EC) *(Quotation attached)*

Figure 16 Keithley Potentiostat 2450-EC

The 2450-EC Electrochemistry Lab System is Keithley's low cost alternative to traditional electrochemistry potentiostats. The 2450-EC brings speed, flexibility, and simplicity right to your fingertips. Its innovative graphical user interface (GUI) and advanced, capacitive touchscreen technology allow intuitive usage and minimize the learning curve to enable researchers, scientists, and students to learn faster, work smarter, and invent easier. The 2450-EC is a versatile instrument, particularly well-suited for research and development in

fundamental electrochemical lab research, characterizing the next generation of materials and electrolytes, new energy storage devices, and faster, smaller sensors.
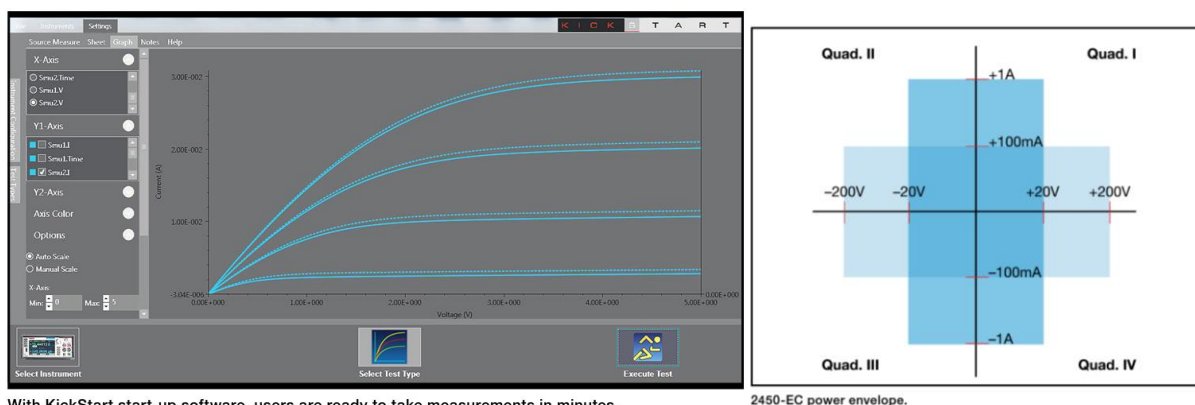
With KickStart start-up software, users are ready to take measurements in minutes.

2450-EC power envelope.

Figure 17 *Kickstart software interface (Left); 2450-EC power envelope [working range] (Right)*

While potentiostats are excellent instruments for electrochemistry applications, they typically lack any front panel display and control knobs, often are 2-quadrant systems only, and must be completely controlled by a computer with software that is not always open for users to customize tests beyond what the software can do. Keithley's 2450-EC is a smart alternative as a DC/low frequency potentiostat. The 2450-EC has features that, in many cases, can perform as well as a potentiostat at lower cost including a wide range of voltages and currents for sourcing or measuring, nV / fA sensitivities, and high impedance sense leads with a typical input resistance of 50G ohms and only 1pA of input bias current, typically acceptable with a wide variety of reference electrodes. The 2450-EC can run internal application test scripts so electrochemistry meaurements can be run without the use of an external computer. Results (graphs) are immediately displayed right on the instrument front panel touchscreen. Connecting the 2450-EC to a 2-, 3-, or 4-electrode cell to perform the same tests as a potentiostat is simple with the included translation cable.

4.1.1 Specification

Voltage Specifications[1,7]

		Source			Measure[2]	
Range	Resolution	Accuracy (23° ±5°C) 1 Year ±(% setting + volts)	Noise (RMS) (<10Hz)	Resolution	Input Resistance	Accuracy (23° ±5°C) 1 Year ±(% rdg. + volts)
20.00000 mV	500 nV	0.100% + 200 µV	1 µV	10 nV	>10 GΩ	0.100% + 150 µV
200.0000 mV	5 µV	0.015% + 200 µV	1 µV	100 nV	>10 GΩ	0.012% + 200 µV
2.000000 V	50 µV	0.020% + 300 µV	10 µV	1 µV	>10 GΩ	0.012% + 300 µV
20.00000 V	500 µV	0.015% + 2.4 mV	100 µV	10 µV	>10 GΩ	0.015% + 1 mV
200.0000 V	5 mV	0.015% + 24 mV	1 mV	100 µV	>10 GΩ	0.015% + 10 mV

Current Specifications[1,7]

		Source			Measure[2]	
Range	Resolution	Accuracy (23° ±5°C)[3] 1 Year ±(% setting + amps)	Noise (RMS) (<10Hz)	Resolution	Voltage Burden	Accuracy (23° ±5°C) 1 Year ±(% rdg. + amps)
10.00000 nA[4]	500 fA	0.100% + 100 pA	500 fA	10 fA	<100 µV	0.10% + 50 pA
100.0000 nA[4]	5 pA	0.060% + 150 pA	500 fA	100 fA	<100 µV	0.060% + 100 pA
1.000000 µA	50 pA	0.025% + 400 pA	5 pA	1 pA	<100 µV	0.025% + 300 pA
10.00000 µA	500 pA	0.025% + 1.5 nA	40 pA	10 pA	<100 µV	0.025% + 700 pA
100.0000 µA	5 nA	0.020% + 15 nA	400 pA	100 pA	<100 µV	0.02% + 6 nA
1.000000 mA	50 nA	0.020% + 150 nA	5 nA	1 nA	<100 µV	0.02% + 60 nA
10.00000 mA	500 nA	0.020% + 1.5 µA	40 nA	10 nA	<100 µV	0.02% + 600 nA
100.0000 mA	5 µA	0.025% + 15 µA	100 nA	100 nA	<100 µV	0.025% + 6 µA
1.000000 A	50 µA	0.067% + 900 µA	3 µA	1 µA	<100 µV	0.03% + 500 µA

4.1.2 Justification

Available setup

Figure 18 *Currently available setup in our lab*

Above mentioned is the currently available setup in the research lab (NML). As clearly mentioned in Fig.??, only a linear potential is achievable in the given setup (300 V without precise current [5 A] and 60 V with precise current [1.5 A]). Thus only Mild Anodization is possible, no variable current with respect to potential can be initiated and no pluse variation can be carried out to develop AAO templates on substrates with modified nanochannels. Thus the need of the keithley 2450-EC potentiostat is high. In addition to varied anodization, if procured, the equipment can also be used to carry out highly sensitive resistance vs time studies in a two or four probe system for gas sensing for vapour gases. It can be used to study the I-V characteristics of a perovskite solar cells layer (FAPbI$_3$/MAPbI$_3$) and also the study the switching application of tellurium based chalcogenide glasses (Se-Te-In).

Thus, the equipment can be used for not only for anodization but also for the study of all the applications currently carried out by the scholars in the lab.

4.2 CH Instruments Electrochemical Analyzer/Workstation (CHI608E/CHI660E)
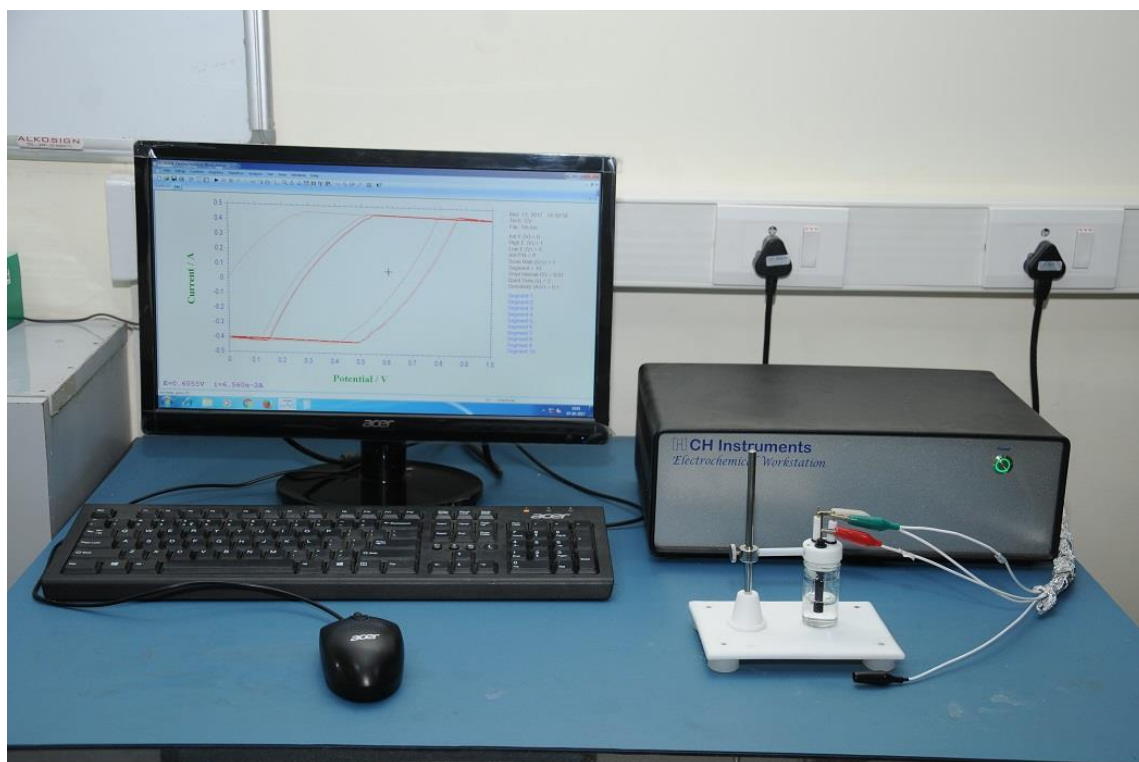
(Quotation included)

Figure 19 CH Instruments Electrochemical Workstation/Analyzer

The Model 600E series is designed for general purpose electrochemical measurements. The system contains a fast digital function generator, a direct digital synthesizer for high frequency AC waveforms, high speed dual-channel data acquisition circuitry, a potentiostat, and a galvanostat (available only in select models). The potential control range is ±10 V and the current range is ±250 mA. The instrument is capable of measuring current down to picoamperes. The instrument is very fast. The function generator can update at a 10 MHz rate. Two high speed and high resolution data acquisition channels allow both current and potential (or an external voltage signal) to be sampled simultaneously at a rate of 1 MHz, with 16-bit resolution. The instrument provides a very wide dynamic range of experimental time scales. For instance, the scan rate in cyclic voltammetry can be up to 1000 V/s with a 0.1 mV potential increment or 5000 V/s with a 1 mV potential increment. The potentiostat / galvanostat uses a 4- electrode configuration, allowing it to be used for liquid/liquid interface measurements, and eliminating the effect of the contact resistance of connectors and relays for high current measurements. The data acquisition systems also allow an external input signal (such as spectroscopic) to be recorded simultaneously during an electrochemical measurement.

The instrument is capable of a wide variety of electrochemical techniques, and is available with integrated simulation and fitting software functions for both impedance and cyclic voltammetry. These features provide powerful tools for both electrochemical mechanistic studies and trace analysis.

4.2.1 *Specification*

Potentiostat:

• Zero resistance ammeter • 2- or 3- or 4-electrode configuration • Floating (isolated from earth) or earth ground • Maximum potential: ±10 V • Maximum current: ±250 mA continuous, ±350 mA peak • Compliance Voltage: ±13 V • Potentiostat rise time: < 1 μs, 0.8 μs typical •

Potentiostat bandwidth (-3 dB): 1 MHz • Applied potential ranges: ±10 mV, ±50 mV, ±100 mV, ±650 mV, ±3.276 V, ±6.553 V, ±10 V • Applied potential resolution: 0.0015% of potential range • Applied potential accuracy: ±1 mV, ±0.01% of scale • Applied potential noise: < 10 µV rms • Measured current range: ±10 pA to ±0.25 A in 12 ranges • Measured current resolution: 0.0015% of current range, minimum 0.3 fA • Current measurement accuracy: 0.2% if current range >=1e-6 A/V, 1% otherwise • Input bias current: < 20 pA

Galvanostat:

• Galvanostat applied current range: 3 nA – 250 mA • Applied current accuracy: 20 pA ±0.2% if > 3e-7A, ±1% otherwise • Applied current resolution: 0.03% of applied current range • Measured potential range: ±0.025 V, ±0.1 V, ±0.25 V, ±1 V, ±2.5 V, ±10 V • Measured potential resolution: 0.0015% of measured range

Electrometer:

• Reference electrode input impedance: 1e12 ohm • Reference electrode input bandwidth: 10 MHz • Reference electrode input bias current: <= 10 pA @ 25°C

Waveform Generation and Data Acquisition:

• Fast waveform update: 10 MHz @ 16-bit • Fast data acquisition: dual channel 16-bit ADC, 1,000,000 samples/sec simultaneously • External signal recording channel at maximum 1 MHz sampling rate

Experimental Parameters:

• CV and LSV scan rate: 0.000001 to 10,000 V/s • Potential increment during scan: 0.1 mV @ 1,000 V/s • CA and CC pulse width: 0.0001 to 1000 sec • CA and CC minimum sample interval: 1 µs • True integrator for CC • DPV and NPV pulse width: 0.001 to 10 sec • SWV frequency: 1 to 100 kHz • i-t sample interval: minimum 1 µs • ACV frequency: 0.1 to 10 kHz • SHACV frequency: 0.1 to 5 kHz • FTACV frequency: 0.1 to 50 Hz, simultaneously acquire 1st, 2nd,

3rd, 4th, 5th, and 6th harmonics ACV data • IMP frequency: 0.00001 to 1 MHz • IMP amplitude: 0.00001 V to 0.7 V rms

Other Features:

• Automatic and manual iR compensation • Current measurement bias: full range with 16-bit resolution, 0.003% accuracy • Potential measurement bias: ±10V with 16-bit resolution, 0.003% accuracy • External potential input • Potential and current analog output • Programmable potential filter cutoff: 1.5 MHz, 150 KHz, 15 KHz, 1.5 KHz, 150 Hz, 15 Hz, 1.5 Hz, 0.15 Hz • Programmable signal filter cutoff: 1.5 MHz, 150 KHz, 15 KHz, 1.5 KHz, 150 Hz, 15 Hz, 1.5 Hz, 0.15 Hz • RDE control output (Model 630E and up): 0-10V (corresponding to 0-10000 rpm), 16-bit, 0.003% accuracy • Digital input/output lines programmable through macro command • Flash memory for quick software update • Serial port or USB port selectable for data communication • Cell control: purge, stir, knock • CV simulation and fitting program, user-defined mechanisms • Impedance simulation and fitting program • Maximum data length: 256K-16384K selectable • Dimensions: 14.25"(W) × 9.25"(D) × 4.75"(H) • Weight: 12 lb.

4.2.2 Justification

With the growing trend in the research field, the need to purse current topics is of greater need. This equipment mentioned above will help use to explore various possibilities in the field of energy storage and harvesting in a greater level.

This equipment if purchased, will allow us to study and examine materials <u>for electrochemical water splitting *(hydrogen production)* from fresh water and also from sea water *(main objective)*</u>. It can also be used to study various energy based applications like <u>supercapacitors, battery, supercapattery, bio sensor, fuel cells, carbon capture, photoelectrochemical degradation, photoelectrochemical water splitting, corrosion studies, electrodeposition</u> and so on.

These equipment will help us in evaluating the device fabricated and will help us in publishing papers in high impact factor Q1 journals as the need for research in energy harvesting and storage of renewable energy is very high.

These equipment will improve the standards of the research lab and will enable the students to try innovative ideas and subject them to test for bringing out quality research contributions to the society.

These equipment can also push the scholars in preparing devices and trying to publish patents and glorify the name of the institution.

5. SUMMARY

It is proposed to undertake systematic research investigation into the development of AAO template on a substrate and trying to develop nanostructured arrays over the template for hydrogen production. Optimizing the AAO template on the substrate will be carried out in the lab and varied structures in the AAO channels will also be tried. These processes are carried out to achieving a device with nanostructured array of desired material over a conducting substrate like ITO/FTO glass for water splitting application. This activity is also deemed to be optimized in laboratory conditions and then up-scaled to industrial grade also. Initiatives will be taken to test the achieved device using a commercial solar cell and the renewable current produces will be stored as hydrogen which can be used later for energy production through fuel cells and the by product will be water making it an eco-friendly approach. Then required equipment's to achieve this level of research are been stated and their needs have been justified above. In addition the quotation for these equipment have also been attached along with this document for reference purposes. Additional innovative ideas have also been state which can bring about ground-breaking research output with the equipment's requested, if carried out it

will bring laurels to the department and the institution along with high impact factor publications.

REFERNECES

[1]   Anantharaj S, Ede SR, Karthick K, Sam Sankar S, Sangeetha K, Karthik PE, et al. Precision and correctness in the evaluation of electrocatalytic water splitting: Revisiting activity parameters with a critical assessment. Energy Environ Sci 2018;11:744–71. https://doi.org/10.1039/c7ee03457a.

[2]   Patel M, Park WH, Ray A, Kim J, Lee JH. Photoelectrocatalytic sea water splitting using Kirkendall diffusion grown functional Co_3O_4 film. Sol Energy Mater Sol Cells 2017;171:267–74. https://doi.org/10.1016/j.solmat.2017.06.058.

[3]   Talapaneni SN, Singh G, Kim IY, AlBahily K, Al-Muhtaseb AH, Karakoti AS, et al. Nanostructured Carbon Nitrides for CO2 Capture and Conversion. Adv Mater 2020;32:1–21. https://doi.org/10.1002/adma.201904635.

[4]   Zheng Z, Qiao Y, Cai Y, He Y, Tang Y, Li L. MoS2 decorated CdS hybrid heterojunction for enhanced photoelectrocatalytic performance under visible light irradiation. J Colloid Interface Sci 2019;533:561–8. https://doi.org/10.1016/j.jcis.2018.08.078.

[5]   Thai NX, Van Duy N, Van Toan N, Hung CM, Van Hieu N, Hoa ND. Effective monitoring and classification of hydrogen and ammonia gases with a bilayer Pt/SnO_2 thin film sensor. Int J Hydrogen Energy 2020;45:2418–28. https://doi.org/10.1016/j.ijhydene.2019.11.072.

[6]   Dziubaniuk M, Bujakiewicz-Korońska R, Suchanicz J, Wyrwa J, Rękas M. Application of bismuth ferrite protonic conductor for ammonia gas detection. Sensors Actuators, B Chem 2013;188:957–64. https://doi.org/10.1016/j.snb.2013.08.020.

[7]   Hernandez SC, Chaudhuri D, Chen W, Myung N V., Mulchandani A. Single polypyrrole nanowire ammonia gas sensor. Electroanalysis 2007;19:2125–30. https://doi.org/10.1002/elan.200703933.

[8]   Ebrahimi A, Dak P, Salm E, Dash S, Garimella S V., Bashir R, et al. Nanotextured superhydrophobic electrodes enable detection of attomolar-scale DNA concentration within a droplet by non-faradaic impedance spectroscopy. Lab Chip 2013;13:4248. https://doi.org/10.1039/c3lc50517k.

[9]   Mayorga-Martinez CC, Chamorro-Garcia A, Merkoçi A. Electrochemical Impedance Spectroscopy (bio)sensing through hydrogen evolution reaction induced by gold nanoparticles. Biosens Bioelectron 2015;67:53–8. https://doi.org/10.1016/j.bios.2014.05.066.

[10]   Anusha JR, Kim H, Fleming AT, Das SJ, Yu K, Chul B, et al. Sensors and Actuators B : Chemical Simple fabrication of ZnO / Pt / chitosan electrode for enzymatic glucose biosensor. Sensors Actuators B Chem 2014;202:827–33. https://doi.org/10.1016/j.snb.2014.06.024.

[11]   Raj CJ, Kim BC, Cho WJ, Lee WG, Jung SD, Kim YH, et al. Highly Flexible and Planar

Supercapacitors Using Graphite Flakes/Polypyrrole in Polymer Lapping Film. ACS Appl Mater Interfaces 2015;7:13405–14. https://doi.org/10.1021/acsami.5b02070.

[12] Hu Q, Tang M, He M, Jiang N, Xu C, Lin D, et al. Core-shell MnO_2@CoS nanosheets with oxygen vacancies for high-performance supercapattery. J Power Sources 2020;446:227335. https://doi.org/10.1016/j.jpowsour.2019.227335.

[13] Zhang Y, Li P, Yang X, Fa W, Ge S. High-efficiency and stable alloyed nickel based electrodes for hydrogen evolution by seawater splitting. J Alloys Compd 2018;732:248–56. https://doi.org/10.1016/j.jallcom.2017.10.194.

[14] Song F, Hu X. Exfoliation of layered double hydroxides for enhanced oxygen evolution catalysis. Nat Commun 2014;5. https://doi.org/10.1038/ncomms5477.

[15] Niu X, Tang Q, He B, Yang P. Robust and stable ruthenium alloy electrocatalysts for hydrogen evolution by seawater splitting. Electrochim Acta 2016;208:180–7. https://doi.org/10.1016/j.electacta.2016.04.184.

[16] Tafel J. Über die Polarisation bei kathodischer Wasserstoffentwicklung 1905. https://doi.org/https://doi.org/10.1515/zpch-1905-5043.

[17] Dresp S, Dionigi F, Klingenhof M, Strasser P. Direct electrolytic splitting of seawater: Opportunities and challenges. ACS Energy Lett 2019;4:933–42. https://doi.org/10.1021/acsenergylett.9b00220.

[18] Zhang Z, Wang P. Highly stable copper oxide composite as an effective photocathode for water splitting via a facile electrochemical synthesis strategy. J Mater Chem 2012;22:2456–64. https://doi.org/10.1039/c1jm14478b.

[19] Sharma AK, Yewale MA, Chavan GA, Kambale DB, Potdar S. Electrochemical synthesis of nanoplatelets-like $CuS0.2Se_{0.8}$ thin film for photoluminescence applications. Mater Sci Pol 2015;33:397–401. https://doi.org/10.1515/msp-2015-0055.

[20] Li D, Baydoun H, Verani CN, Brock SL. Efficient Water Oxidation Using CoMnP Nanoparticles. J Am Chem Soc 2016;138:4006–9. https://doi.org/10.1021/jacs.6b01543.

[21] Muller GA, Cook JB, Kim HS, Tolbert SH, Dunn B. High performance pseudocapacitor based on 2D layered metal chalcogenide nanocrystals. Nano Lett 2015;15:1911–7. https://doi.org/10.1021/nl504764m.

[22] Jin H, Liu X, Vasileff A, Jiao Y, Zhao Y, Zheng Y, et al. Single-Crystal Nitrogen-Rich Two-Dimensional Mo_5N_6 Nanosheets for Efficient and Stable Seawater Splitting. ACS Nano 2018;12:12761–9. https://doi.org/10.1021/acsnano.8b07841.

[23] Bennett JE. Electrodes for generation of hydrogen and oxygen from seawater. Int J Hydrogen Energy 1980;5:401–8. https://doi.org/10.1016/0360-3199(80)90021-X.

[24] Li Y, Wang R, Li H, Wei X, Feng J, Liu K, et al. Efficient and Stable Photoelectrochemical Seawater Splitting with TiO_2@g-C_3N_4 Nanorod Arrays Decorated by Co-Pi. J Phys Chem C 2015;119:20283–92. https://doi.org/10.1021/acs.jpcc.5b05427.

[25] Wang Z, Xu W, Yu K, Feng Y, Zhu Z. 2D heterogeneous vanadium compound interfacial modulation enhanced synergistic catalytic hydrogen evolution for full pH range seawater splitting. Nanoscale 2020;12:6176–87.

https://doi.org/10.1039/d0nr00207k.

[26] El-Moneim AA. Mn-Mo-W-oxide anodes for oxygen evolution during seawater electrolysis for hydrogen production: Effect of repeated anodic deposition. Int J Hydrogen Energy 2011;36:13398–406. https://doi.org/10.1016/j.ijhydene.2011.07.100.

[27] Sarno M, Ponticorvo E, Scarpa D. Active and stable graphene supporting trimetallic alloy-based electrocatalyst for hydrogen evolution by seawater splitting. Electrochem Commun 2020;111:106647. https://doi.org/10.1016/j.elecom.2019.106647.

[28] Kuang Y, Kenney MJ, Meng Y, Hung WH, Liu Y, Huang JE, et al. Solar-driven, highly sustained splitting of seawater into hydrogen and oxygen fuels. Proc Natl Acad Sci U S A 2019;116:6624–9. https://doi.org/10.1073/pnas.1900556116.

[29] Yu L, Zhu Q, Song S, McElhenny B, Wang D, Wu C, et al. Non-noble metal-nitride based electrocatalysts for high-performance alkaline seawater electrolysis. Nat Commun 2019;10:1–10. https://doi.org/10.1038/s41467-019-13092-7.

[30] Kshirsagar J, Shrivastava R, Adwani P. Preparation and characterization of copper oxide nanoparticles and determination of enhancement in critical heat flux. Therm Sci 2017;21:233–42. https://doi.org/10.2298/TSCI140619026K.

[31] Tran TH, Nguyen VT. Copper Oxide Nanomaterials Prepared by Solution Methods, Some Properties, and Potential Applications: A Brief Review. Int Sch Res Not 2014;2014:1–14. https://doi.org/10.1155/2014/856592.

[32] Rodney JD, Deepapriya S, Robinson MC, Das SJ, Perumal S, Sivakumar P, et al. $Cu_{1-x}RE_xO$ (RE = La, Dy) decorated dendritic CuS nanoarrays for highly efficient splitting of seawater into hydrogen and oxygen fuels. Appl Mater Today 2021;24:101079. https://doi.org/https://doi.org/10.1016/j.apmt.2021.101079.

Quotations for the requested equipment's

CONVERGENT TECHNOLOGIES INDIA PVT LTD. . . . .

QUOTATION

To **NITK** National Institute of Technology Karnataka, Srinivasnagar PO, Surathkal, Mangalore surathkal,Karnataka, India, 575025 Phone No. : 2474000 Kind Attn : Prof. N.K.Udayashankar, Head of Department, Physics	Quotation No. **609/2022** Buyer Ref. No. **Email & discussion** Mode/Term of Payment **100% against delivery** Terms of Delivery **15 to 20 weeks**	Date **15/04/2022** Dispatch Through **Road** Validity **30 days** Incoterms **FOR**

S.No	Part No	Description of Goods	HSN/SAC	Qty	Unit	Unit Rate(INR)	Total (INR)
1	2450-EC	**2450-EC POTENTIOSTAT**		1	Nos	7,75,000.00	7,75,000.00
2	KICKSTARTFL-SUITE	**License; KICKSTARTFL-SUITE for all base apps of KickStart 2.0; Floating**		1	Nos	86,700.00	86,700.00
			Sub Total				8,61,700.00
			GST @ 5.000 %				43,085.00
			Total	2			**9,04,785.00**

Amount Chargeable (in words) : INR Nine Lakh Four Thousand Seven Hundred Eighty Five Only

---

Warranty   1 year. Warranty does not cover accessories, consumables, software etc. Accessories carry 90 days warranty.

Payment   **10**0% against delivery.

Delivery   15 to 20 weeks from receipt of acceptable order.

Order to be placed on:-

Convergent Technologies India Pvt Ltd.
No. 13/1, 5th Block, Railway parallel Road
Kumara Park West, 7th Cross, Central Street
Bangalore -560 020. Ph: 080-46009933, 080-49668031, 080-23460180, 06363990944

email: sales@convergenttech.in
GST No: 29AAGCC4951P1ZZ

For Convergent Technologies India Pvt Ltd

Gururaj N
Account Manager   Mobile: 9844442074
Email:gururaj@convergenttech.in

This is a Computer Generated Document, no signature required

No. 13/1, 5th Block, Railway parallel Road Kumara Park West, 7th Cross, Central Street,Bangalore 560020
Phone No.:080 23670050   E-mail:sales@convergenttech.in   www.convergent-india.com

Page 1 of 1

QUOTATION #NITK/CHI/22/04/037   **Date: - April 13, 2022**

Prof. N. K. Udayashankar
Head, Department of Physics
National Institute of Technology Karnataka
Surathkal – 575025

Sr. No	Model No.	Description	Unit Price (US$)
		CH Instruments Inc., USA	
01.	CHI608E	Electrochemical Workstation with Potentiostat/Galvanostat with Corrosion, Impedance, Electrochemistry s/w, and Latest Windows Based Acquisition s/w also includes power supply 220V/50Hz, Interface Cable for USB Port, Cell Cable, Manuals & Installation.	12,095.00

CHI608E description bullets:

- Cyclic Voltammetry (CV)
- **Linear Sweep Voltammetry Plots**
  Current – E, Linear Pol Res
  Solar Plot (**Isc, Voc, Pwr Max (W), FF, Voltage max (V)**)
  Power – E
- **Tafel Plot (TAFEL), Linear Polarisation**
- Chrono Amperometry (CA)
- Chrono Coulometry (CC)
- Bulk Electrolysis with Coulometry (BE)
- **AC Impedance (IMP) – 10uHz to 1MHz**
- **Impedance – Time (IMPT)**
- **Impedance – Potential (IMPE)**
- **Chronopotentiometry (CP)**
- **Chronopotentiometry with Current Ramp (CPCR)**
- **Multi-Current Steps (ISTEP)**
- **Potentiometer Stripping Analysis (PSA)**
- Open Circuit Potential – Time (OCPT)
- Galvanostat
- Limited version of CV simulator
- Impedance Simulator
- IR Compensation
- External Potential Input
- Auxiliary Signal Measurement Channel

AC Impedance Plots
- Bode : log Z vs log (freq)
- Bode : Phase , vs log (freq)
- Bode : log Z" & Z' vs log (freq)
- Bode : log Y vs log (freq)
- Nyquist ; Z" vs Z'
- 3D Plots
- Admittance; Y" vs Y'
- Warburg: Z" & Z' vs $w^{1/2}$ w-angular frequency
- Z' vs w Z",Z' vs Z"/w
- Cot (phase) vs $w^{1/2}$

Tafel plot (TAFEL) includes
Linear Polarisation, Pitting Corrosion, Noise Measurements, Corrosion current, Potentiodynamic deactivation etc

SINSIL INTERNATIONAL PVT LTD

No.31, Opposite S.J.E.S College
Old Madras Road, Medahalli
Virgonagar Post, Bengaluru – 560 049
www.sinsilinternational.com

Telephone : 080-50891594
Fax : 080-25615369
Mobile : 09341282569
Email : bangalore@sinsil.in

02.	CHIXXX	Electrochemical Cell System includes, 4 glass cells with one Cell top Pt Working Electrode GC Working Electrode Ag/AgCl Reference (aq) Ag/AgCl Reference (non aq) Calomel Reference Electrode Pt Wire Counter Electrode Electrode Polishing Kit & Cell Stand*	950.00
03.	CHI-S/W	**Licensed & Full version of software for Electrochemistry & all the techniques of CHI6xxE.** **Software Features:** 32-bit Windows-based software, Multi-document interface Open, save, delete, list, conversion, and print files Run, macro, iR compensation, filtering, preconditioning, step functions, and cell control Data plot, overlay and parallel plots, Graphics options, color and font selections Smoothing, derivatives, integration, semi-derivative and semi-integral, interpolation, baseline fitting & subtraction, linear baseline correction, data point removing, data point modification, background subtraction, signal averaging, mathematical operation, Fourier spectrum Calibration curve, standard addition, data file report, concentration – time dependence report and plot. Digital simulation, user defined mechanisms Data information.	No-Charge
04.	CHI-S/W-UPG	**UPGRADATION OF SOFTWARE IS FREE OF COST FOR LIFETIME.**	No-Charge
05.	COMP	Desktop Computer with 1TB Hard Disc, 4GB RAM, 18.5" LED Monitor with Standard Configuration.	700.00

Total Ex works, USA	13,745.00
Air Freight & Insurance	500.00
Total CIP Bangalore	US$ 14,245.00

Alternates for Item no.1

01.	CHI660E	Electrochemical Workstation with Potentiostat/Galvanostat with Corrosion, Impedance, Electrochemistry s/w, and Latest Windows Based Acquisition s/w also includes power supply 220V/50Hz, Interface Cable for USB Port, Cell Cable & Installation. **General Techniques** • Cyclic Voltammetry (CV) with simulation/fitting programs • Linear Sweep Voltammetry (LSV) with stripping • Bulk Electrolysis with Coulometry (BE) **Trace Metal analysis & Pulse Techniques** • Differential Pulse Voltammetry (DPV) with stripping • Normal Pulse Voltamemtry (NPV) with stripping • Square Wave-Osteryoung Voltammetry (SWV) with stripping **Corrosion** • Tafel Plot (TAFEL), potentiodynamic deactivation, pitting corrosion, corrosion rate, linear Polarisation, Corrosion current etc.	16,620.00

Regd. Office: 165 Parishram Park, Gorwa, Vadodara-390016   GST NO. 24AAVCS3020N1Z0 Dated 25/06/2017
Vadodara Ph: 09833011933   **email:** info@sinsil.in   **Kolkata**   Ph: 09681442892 **email:** kolkata@sinsil.in
Mumbai   Ph: 09167404043   **email:** mumbai@sinsil.in   **Delhi**   Ph: 09312437300 **email:** delhi@sinsil.in
Chennai   Ph: 09980487123   **email:** bangalore@sinsil.in   **Hyderabad** Ph: 08008999507 **email:** bangalore@sinsil.in
Page 2 of 6

SINSIL INTERNATIONAL PVT LTD

No.31, Opposite S.J.E.S College
Old Madras Road, Medahalli
Virgonagar Post, Bengaluru – 560 049
www.sinsilinternational.com

Telephone : 080-50891594
Fax : 080-25615369
Mobile : 09341282569
Email : bangalore@sinsil.in

Fuel cell
- Multi-Potential Steps (STEP)
- Multi-Current Steps (ISTEP)
- Amperometric i-t Curve (i-t) – Lifetime testing
- Polarisation I-V curves Linear Sweep
- Open Circuit Potential – Time (OCPT)

Impedance
- AC Impedance (IMP)
- Impedance – Time (IMPT) (Mott-Scottsky)
- Impedance – Potential (IMPE)
- Impedance Simulator with fitting
- Open Circuit Potential – Time (OCPT)

AC Impedance Plots with Simulation
- Bode : log Z vs log (freq)
- Bode : P¦hase , vs log (freq)
- Bode : log Z" & Z' vs log (freq)
- Bode : log Y vs log (freq)
- Nyquist ; Z" vs Z'
- Admittance; Y" vs Y'
- Warburg: Z" & Z' vs $w^{1/2}$ w-angular frequency
- Z' vs w Z"
- Z' vs Z"/w
- Cot (phase) vs w $^{1/2}$

Battery Charge/Discharge
- Galvanostatic Charge discharge single/multiple cycle - Chrono Potentiometry (CP) with potential limits, polarity by potential or time, no. of cycles etc
- Voltage vs current density curves

Deposition Studies
Single or Multi potential steps with charge limits, single or Multi current steps, mixed voltage/current control using macro

Photovoltaic studies
I-V measurements, I max, Pmax, Fill factor etc

Insitu Spectroelectrochemical study (optional)
- Transmission mode for ITO plates or Pt grid, Reflection mode for Pt/GC electrodes & Dip probe for coulometrically generated species

General Useful Techniques
- Chrono Amperometry (CA)
- Chrono Coulometry (CC)
- AC Voltammetry (ACV) with stripping
- Differential Normal pulse Voltamemtry (DPNV) with stripping
- Second Harmonic AC Voltammetry (SHACV) with stripping
- Differential Pulse Amperometry (DPA)
- Double Differential Pulse Amperometry (DDPA)
- Triple Pulse Amperometry (TPA)
- Integrated Pulse Amperometry Detection (IAPD)
- Hydrodynamic Modulation Voltammetry (HMV)
- Sweep-Step Functions (SSF)

Regd. Office: 165 Parishram Park, Gorwa, Vadodara-390016   GST NO. 24AAVCS3020N1Z0 Dated 25/06/2017
Vadodara Ph: 09833011933   **email:** info@sinsil.in   **Kolkata**   Ph: 09681442892 **email:** kolkata@sinsil.in
Mumbai   Ph: 09167404043   **email:** mumbai@sinsil.in   **Delhi**   Ph: 09312437300 **email:** delhi@sinsil.in
Chennai   Ph: 09980487123   **email:** bangalore@sinsil.in   **Hyderabad** Ph: 08008999507 **email:** bangalore@sinsil.in

Page 3 of 6

SINSIL INTERNATIONAL PVT LTD

No.31, Opposite S.J.E.S College
Old Madras Road, Medahalli
Virgonagar Post, Bengaluru – 560 049
www.sinsilinternational.com

Telephone : 080-50891594
Fax : 080-25615369
Mobile : 09341282569
Email : bangalore@sinsil.in

		• Chronopotentiometry with Current Ramp (CPCR) • Potentiometric Stripping Analysis (PSA) • Staricase Voltammetry (SCV) with stripping • Auxiliary Signal Measurement Channel • RDE control (0-10V output) • IR Compensation • External Potential Input	

Alternates for item no.2

01.	CHIXXX	Electrochemical Cell System includes, 4 glass cells with Two Cell top, Pt Working Electrode -3 No.s GC Working Electrode -3 No. s Ag/AgCI Reference (aq) -3 No. s Ag/AgCl Reference (non aq) -3 No. s Calomel Reference Electrode -3 No. s Pt Wire Counter Electrode - 3 No. s Electrode Polishing Kit	2,500.00

Optional Accessories

01.	CHI 200B	PicoAmp booster and faraday (upto 1 pA operation for low current measurability)	1,045.00
02.	CHI 680C	AmpBooster upto 2 Amps for higher current measurement	2,495.00
03.	CS-3A	**Cell stand with Faraday Cage with SVC-3.** Input gas line connection is easy and quick. Manual or Remote on-off control of gas purge-blanket. Manual control of gas purge-blanket rate. Manual or remote on-off control of magnetic stirrer. Adjustments of magnetic stirrer rate are controlled manually. Voltammetry cell cap. Small volume glass cell vials. Mounted cell top compatible with electro-chemical accessories. The SVC-3 cell comes with one counter electrode, one Teflon cap and 7 glass vials. By using this cell user can run experiments free from gasification steam. Also researchers can get rid of influence of oxygen in the cell by bubbling nitrogen gas. This SVC-3 feature is well suited for measurement of ultra-weak current.	2,900.00

Regd. Office: 165 Parishram Park, Gorwa, Vadodara-390016   GST NO. 24AAVCS3020N1Z0 Dated 25/06/2017
Vadodara Ph: 09833011933   **email:** info@sinsil.in   **Kolkata**   Ph: 09681442892 **email:** kolkata@sinsil.in
Mumbai   Ph: 09167404043   **email:** mumbai@sinsil.in   **Delhi**   Ph: 09312437300 **email:** delhi@sinsil.in
Chennai   Ph: 09980487123   **email:** bangalore@sinsil.in   **Hyderabad** Ph: 08008999507 **email:** bangalore@sinsil.in
Page 4 of 6

SINSIL INTERNATIONAL PVT LTD

No.31, Opposite S.J.E.S College
Old Madras Road, Medahalli
Virgonagar Post, Bengaluru – 560 049
www.sinsilinternational.com

Telephone : 080-50891594
Fax : 080-25615369
Mobile : 09341282569
Email : bangalore@sinsil.in

Terms & Conditions: -

01. PO: In favour of CH Instruments Inc., USA through Sinsil International Pvt Ltd.

02. Payment: Wire Transfer In favour of CH Instruments Inc., USA

Address: -

CH Instruments, Inc.
3700 Tennison Hill Drive, Austin, TX 78738, USA
Tel: (512) 402-0176, Fax: (512) 402-0186
E-mail: info@chinstruments.com

Bank Details: -

Swift code   : CHASUS33
ABA #   : 111000614
Account Number : 265755839
Account Name   : CH Instruments, Inc.
Bank Name   : JPMorgan Chase Bank, N.A.
                    12222 Research Blvd
                    Austin, TX 78759   U.S.A.
                    Tel: (512) 219-4452

03. Validity   : 90 days.

04. Delivery   : 6 - 8 Weeks.

05. Warranty   : 1 year.

06. Customs Duty & Clearance Charges are as applicable & are borne by the purchaser.

07. Computer System & Cell Stand to be supplied by Sinsil International locally.

08. Installation is done by Sinsil International Engineers.

09. There is no element of agency commission is involved in this quotation.

For SINSIL INTERNATIONAL PVT LTD.

Vijaykumar B
Sales & Service Engineer
9591360386

Regd. Office: 165 Parishram Park, Gorwa, Vadodara-390016
Vadodara Ph: 09833011933   **email:** info@sinsil.in
Mumbai   Ph: 09167404043   **email:** mumbai@sinsil.in
Chennai   Ph: 09980487123   **email:** bangalore@sinsil.in

GST NO. 24AAVCS3020N1Z0 Dated 25/06/2017
Kolkata   Ph: 09681442892 **email:** kolkata@sinsil.in
Delhi   Ph: 09312437300 **email:** delhi@sinsil.in
Hyderabad Ph: 08008999507 **email:** bangalore@sinsil.in

Page 5 of 6

Date: - April 13, 2022

Prof. N. K. Udayashankar
Head, Department of Physics
National Institute of Technology Karnataka
Surathkal – 575025

Dear Sir / Madam,

Thank you for your Enquiry,

As per your request enclosed please find the quotation for,

CH Instruments Inc., USA, Electrochemical Workstation with EIS.

Kindly go through the same and get back to us for any further information / clarifications.

Thanking you and assuring you of our best attention and services all the time.

For SINSIL INTERNATIONAL PVT LTD.

Vijaykumar B
Sales & Service Engineer
9591360386

Regd. Office: 165 Parishram Park, Gorwa, Vadodara-390016   GST NO. 24AAVCS3020N1Z0 Dated 25/06/2017
Vadodara Ph: 09833011933   **email:** info@sinsil.in   **Kolkata**   Ph: 09681442892 **email:** kolkata@sinsil.in
Mumbai   Ph: 09167404043   **email:** mumbai@sinsil.in   **Delhi**   Ph: 09312437300 **email:** delhi@sinsil.in
Chennai   Ph: 09980487123   **email:** bangalore@sinsil.in   **Hyderabad** Ph: 08008999507 **email:** bangalore@sinsil.in
Page 6 of 6